

Human Embryonic Stem Cell Detection by Spatial Information and Mixture of Gaussians

Benjamin Xueqi Guan, Bir Bhanu, Ninad Thakoor
Electrical Engineering
University of California, Riverside
Riverside, USA
Email: {xguan001, bhanu, nthakoor}@ee.ucr.edu

Prudence Talbot, Sabrina Lin
Cell Biology and Neuroscience
University of California, Riverside
Riverside, USA
Email: {prudence.talbot, sabrina.lin}@ucr.edu

Abstract—Human Embryonic Stem Cells (HESCs) possess the potential to provide treatments for cancer, Parkinson’s disease, Huntington’s disease, Type 1 diabetes mellitus etc. Consequently, HESCs are often used in the biological assay to study the effects of chemical agents in the human body. However, detection of HESC is often a challenge in phase contrast images. To improve the accuracy of HESC colony detection, we combine spatial information and the outcome of a mixture of Gaussians model. While a mixture of Gaussians generates reasonable labels for various regions of HESC images, it lacks spatial details and connectivity. Sets of spatially consistent candidate labeling are generated by median filtering the image at different scales followed by thresholding. An optimal combination of filter scale and threshold which maximizes the correlation coefficient between the spatial information and the mixture of Gaussians output is obtained. The paper validates the method for various HESC videos.

Keywords- Apoptosis, Cell Detection, Human Embryonic Stem Cell, Expectation-Maximization Algorithm, Mixture of Gaussians, Spatial Information.

I. INTRODUCTION

Biologists often use noninvasive microscopy imaging technique such as phase contrast imaging to study living biological specimens and to learn about their behavior [1]. This paper focuses on Human Embryonic Stem Cell (HESC) phase contrast images taken from the BioStation IM [2]. The HESC has the capacity to differentiate into diverse human cell types. With the aforementioned characteristic, it is well known that HESCs have the potential to be used in cell replacement therapies for the treatment of human diseases [3]. Subsequently, biologists need to study the HESCs more closely under different chemical conditions in large data sets. However, the study of large volume of data is strenuous and laborious for a human. Therefore, biologists need a good tracking technique to understand the behavior of the stem cells over time. Towards developing an automated stem cell tracking system, cell detection plays an important role. However, there are a number of challenges that make the cell detection challenging: (1) the low signal-to-noise ratio of the phase contrast microscopy images; (2) the topological complexity of cell shapes; and (3) the low

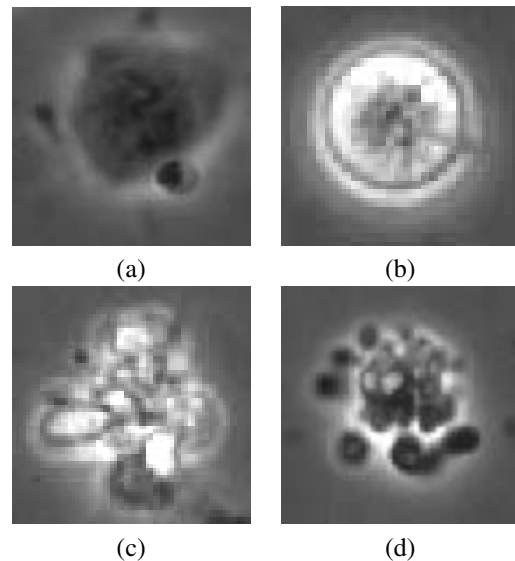


Figure 1: Cell types: (a) Substrate-attached cell, (b) Single unattached cell, (c) Cell undergoing apoptosis, (d) Cell undergoing pre-attachment behavior.

rate of change in intensity between cell and background regions [4].

In HESC phase contrast images, there are four different cell regions: the substrate-attached cells, unattached cells, cells going through apoptosis/cell death and cells with pre-attachment behavior. The four cell types are shown in Fig. 1. The substrate-attached cells are similar to the background in intensity and are usually surrounded by a low intensity halo. The unattached cells are brighter and are similar to the halo in intensity. Cells that are going through apoptosis are blebbing [5] randomly and are brighter. In contrast, the cells that are going through pre-attachment behavior are darker when blebbing and are surrounded by a recognizable halo that distinguishes the cell from the background. Although an individual cell can be in the frame by itself, any combination (homogeneous or heterogeneous) of the above four types of cells can come together to form a cell colony. The cell colony inherently has all the characteristic of the cells. As

seen in Fig. 1(a), the detection for substrate-attached cells and cell colonies that consist of substrate-attached cells is harder than the detection for other type of cells and cell colonies. As a result, a method for accurate detection of substrate-attached cells or colony that consist of substrate-attached cells is needed. In this paper, a combination of spatial information and a mixture of Gaussians, which improves detection accuracy of the cell regions, is introduced.

II. RELATED WORK AND CONTRIBUTIONS

Previous works have shown approaches for cell region detection in phase contrast images [4], [6]. Ambriz-Colin et al. [6] discuss two methods for cell region detection: detection by pixels intensity variance (PIV) and by gray level morphological gradient (GLMG). The PIV method performs pixel classification on the normalized image. It recognizes the probable cell regions and labels the rest as the background in the normalized image. The GLMG method detects the cell regions by using morphological gradient that is calculated from the dilation and erosion operations, and by a threshold that separates the pixels belonging to a cell and to the background. Li et al. [4] also mention a combined use of morphological rolling-ball filtering and a Bayesian Classifier that is based on the estimated cell and background gray scale histograms to classify the image pixels into either the cell regions or the background.

We suggest using spatial information and the result from the mixture of Gaussians model to estimate the cell regions. The mixture of Gaussians provides an estimate for various cell regions. However, it lacks spatial consistency as the cell region intensities lie on both lower and higher side of the background intensities. We generate spatial information for the image first. The result from the mixture of Gaussians is then used to estimate the optimal threshold to segment the spatial information into cell regions and background.

III. TECHNICAL APPROACH

In this section, we formulate the HESC detection and analysis process. The overview of the process is shown in Fig. 2.

A. Motivation and Problem Formulation

Cell lineage analysis is a popular technique to learn about cell behavior through tracking. In order to track the cells, the accurate detection of the cell regions is essential. To improve the accuracy and consistency in the detection of cell regions, a reliable detection technique for HESC phase contrast image is needed. To formulate our approach, we enlist important properties about the HESC images.

- The intensity of the substrate region is locally constant while in the cell regions, the intensity varies locally.
- The images can be split into three distinct areas based on their intensities:
 - A. Substrate-attached cells (the darkest regions),

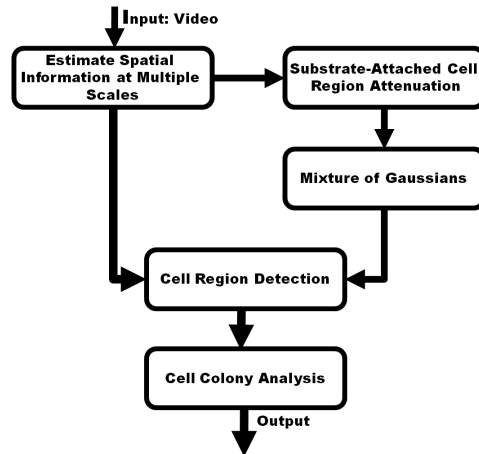


Figure 2: Human Embryonic Stem Cell Detection and Analysis Process.

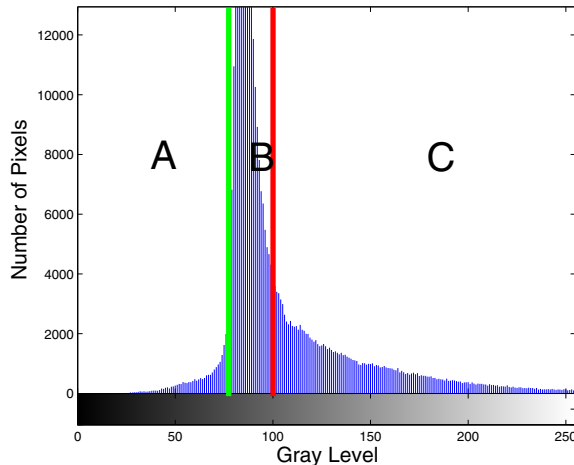


Figure 3: A typical HESC image histogram with regions of interest

- B. Substrate (intensities in the middle),
- C. Halo (the brightest regions).

Figure 3 shows the histogram of a typical HESC image, which is divided into three regions. Region A is the substrate-attached cell region, Region B is the substrate region and Region C is the halo region. Our method uses the local spatial information as well as the intensity information to estimate cell regions. The mixture of Gaussians is an intensity based approach and only provides part of the cell regions. Therefore, we utilize the spatial information to recover the missing regions.

B. Estimating Spatial Information

The input image contains the spatial information that can be used to distinguish the cell regions from the substrate. We apply combination of median filtering to separate these regions. A spatial information image I_S at scale m is

estimated as,

$$I_S(m) = \text{med}(\text{abs}(I - \text{med}(I, m)), m + 2) \quad (1)$$

where $\text{med}(\cdot, s)$ denotes the median filtering operation with window size s and I is the original image. The operation $\text{abs}(I - \text{med}(I, m))$ yields low values in the area with constant local intensity (i.e., substrate) and high values in areas with varying intensities (i.e. cell regions). The larger median filter smooths interior cell regions while preserving the edges. Unlike the original image which has three intensity modes, the spatial information image is bimodal. Thus, a single threshold can be used to separate the substrate and cell regions. However, one still has to select appropriate threshold T and scale m .

With the estimated spatial information, I_S from equation (1), we can choose the spatial information with a specific window size to selectively attenuate the input image for the mixture of Gaussians which follows. We normalize the spatial information at location (r, c) as,

$$I_{MS}(r, c) = 1 - \frac{I_S(r, c)}{\max(I_S)} \quad (2)$$

I_{MS} is then used to attenuate the original image:

$$I_G(r, c) = I(r, c) \times I_{MS}(r, c) \quad (3)$$

I_G is the attenuated image that is used as the input image to the mixture of Gaussians. The attenuation affects both substrate-attached cells and halo regions. It creates more separation between substrate and substrate-attached cells. Although halo regions undergo undesired attenuation, the effect is minimal due to the high contrast between the substrate and halo regions. Fig. 4 (c) shows the effect of selective attenuation.

C. Mixture of Gaussians

The HESC phase contrast images have three regions of interest: the substrate-attached cell region, the substrate and the halo region. Thus, a mixture of three Gaussians [7] is used to estimate the probable cell regions. The expectation maximization (EM) algorithm [8] is used to estimate the parameters $\theta = \{\theta_1, \theta_2, \dots, \theta_L\}$ of the mixture of L Gaussians. θ_i is a vector of weight w_i , mean μ_i and standard deviation σ_i for the i th component of the mixture. The EM algorithm is used to maximize the likelihood of three regions of interest: the substrate-attached cell regions, the substrate and the halo regions. The probability that pixel located at (r, c) belongs to i th component of mixture can be written as,

$$P_i(r, c) = \frac{1}{\sigma_i \sqrt{2\pi}} \exp \left\{ \frac{-(I_G(r, c) - \mu_i)^2}{2\sigma_i^2} \right\} \quad (4)$$

where I_G is an $M \times N$ image to be modeled by the mixture of Gaussians. With a known P_i , the membership

probabilities F_i can be estimated as,

$$F_i(r, c) = \frac{w_i P_i(r, c)}{\sum_{k=1}^L w_k P_k(r, c)} \quad (5)$$

The membership probabilities are then used to update θ^n in the n th iteration. The weights, means and standard deviations at each iteration are updated by,

$$w_i = \frac{1}{M \times N} \sum_{r=1}^M \sum_{c=1}^N F_i(r, c) \quad (6)$$

$$\mu_i = \frac{\sum_{r=1}^M \sum_{c=1}^N F_i(r, c) I_G(r, c)}{\sum_{r=1}^M \sum_{c=1}^N F_i(r, c)} \quad (7)$$

$$\sigma_i = \sqrt{\frac{\sum_{r=1}^M \sum_{c=1}^N F_i(r, c) (I_G(r, c) - \mu_i)^2}{\sum_{r=1}^M \sum_{c=1}^N F_i(r, c)}} \quad (8)$$

The process is repeated until convergence which means that the absolute change between θ^n and θ^{n-1} is lesser than a small user defined value [9]. After convergence, each pixel is assigned to the region with maximum membership probability.

Figures 5(a) to (c) show the membership probabilities of each region of interest for one of the images. The brighter means higher membership probability while darker represents a lower membership probability.

After the mixture of Gaussians segmentation, we can improve the detection of the substrate-attached cell regions with region growing. The conventional region growing cannot capture the substrate-attached cell regions as their intensity and substrate intensity are similar. Therefore, we need to add the spatial knowledge to attenuate the pixel intensity near the substrate-attached cell regions.

$$I_M(r, c) = I_G(r, c) - I_G(r, c) \exp(-I_D(r, c)) \quad (9)$$

where I_D is a Euclidean distance transform of the substrate-attached cell regions. The effect of equation (9) is shown in Fig. 6(b). The local information used in equation (9) helps detecting the substrate-attached cell regions that conventional region growing would miss. After the region growing, grown substrate-attached cell regions and halo regions are combined to form the probable cell regions. The rest of the image is labeled as the substrate.

D. Cell Region Detection

Although the cell regions found by mixture of Gaussians lack the spatial details and connectivity, it provides a good template for the actual cell regions. On the other hand, the spatial information images retain spatial details and connectivity. However, each combination of a threshold T and a scale m results in a different detection. Depending on the value of m , the image might be under- or over-smoothed. If threshold is too high or too low, the cell region would be recognized incorrectly. To overcome these problems, we

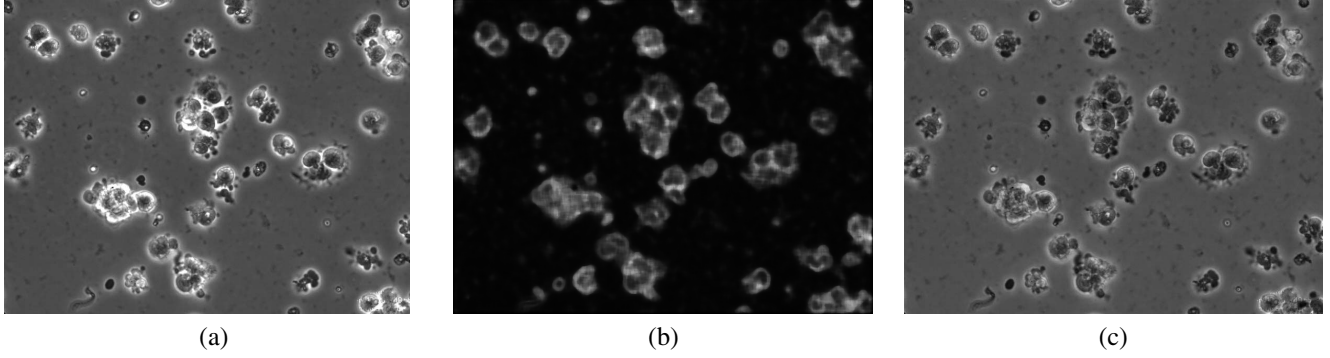


Figure 4: Selective attenuation: (a) Original Image, (b) Spatial information image, (c) Selective attenuation on (a).

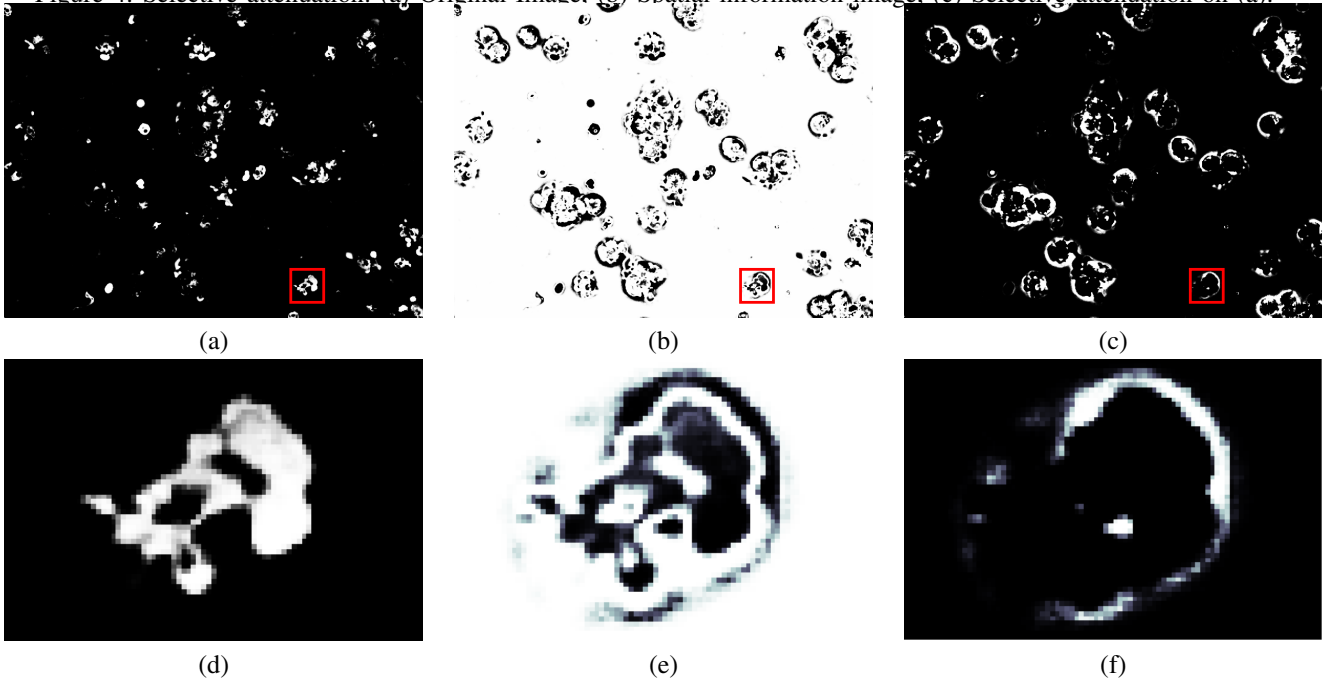


Figure 5: Probability map: (a) Membership probability for substrate-attached cell regions, (b) Membership probability for the substrate, (c) Membership probability for halo, (d)(e)(f) Detailed views of a cell region in (a),(b),(c) respectively

compare thresholded spatial information images with the outcome of mixture of Gaussians.

We first estimate spatial information image at specific scale m . Then we calculate the correlation coefficient of the spatial information image $I_S(m)$ thresholded at different values and the probable cell regions after the mixture of Gaussians. We obtain the optimal threshold that yields the maximum correlation coefficient value. A set of maximum correlation values are found by varying the scale m . The optimal solution can be determined by finding the maximum correlation coefficient value that yields a lowest variance across scale values m .

E. Cell Colony Analysis

The last step is to further break down the detected cell colony regions into individual cell regions. In order to detect the individual cell regions, a marker based watershed tech-

nique is used [10]. The marker is estimated by performing mixture of two Gaussians on the image data within the detected cell colony regions. The boundaries that separate the background and the cell colony regions are also imposed on the process. The process produces many probable cell regions. Those regions are the result of the watershed's over-segmentation, and it can be solved by creating an entropy table. The entropy table contains the entropy values of the individual cell regions as well as the entropy when one of the neighbors of the cell region is considered as a part of the cell region. We combine each small region with its neighbor for which the merge causes the lowest entropy change. The result of cell colony analysis is shown in Fig. 7.

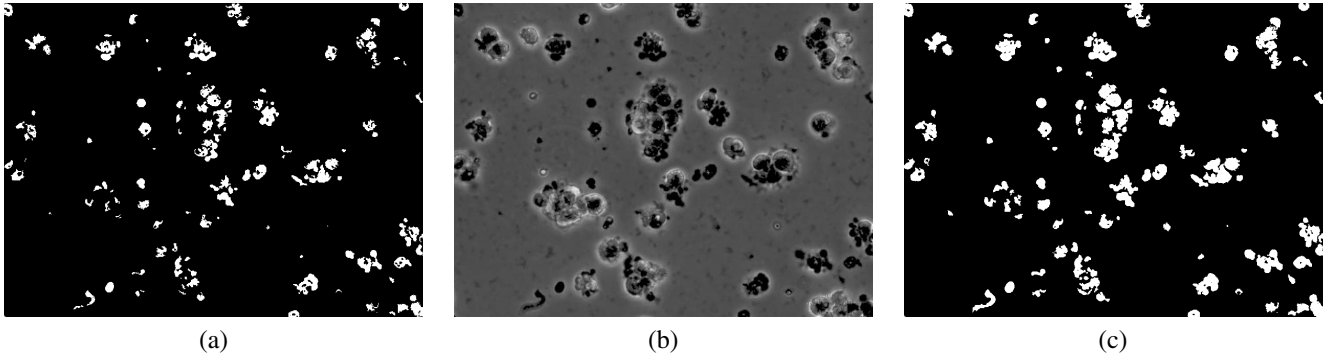


Figure 6: Substrate-attached cell region growing: (a) Conventional region growing of substrate-attached cell regions, (b) Image attenuated by Eqn. (9), (c) Result of modified region growing with (b) as the input.

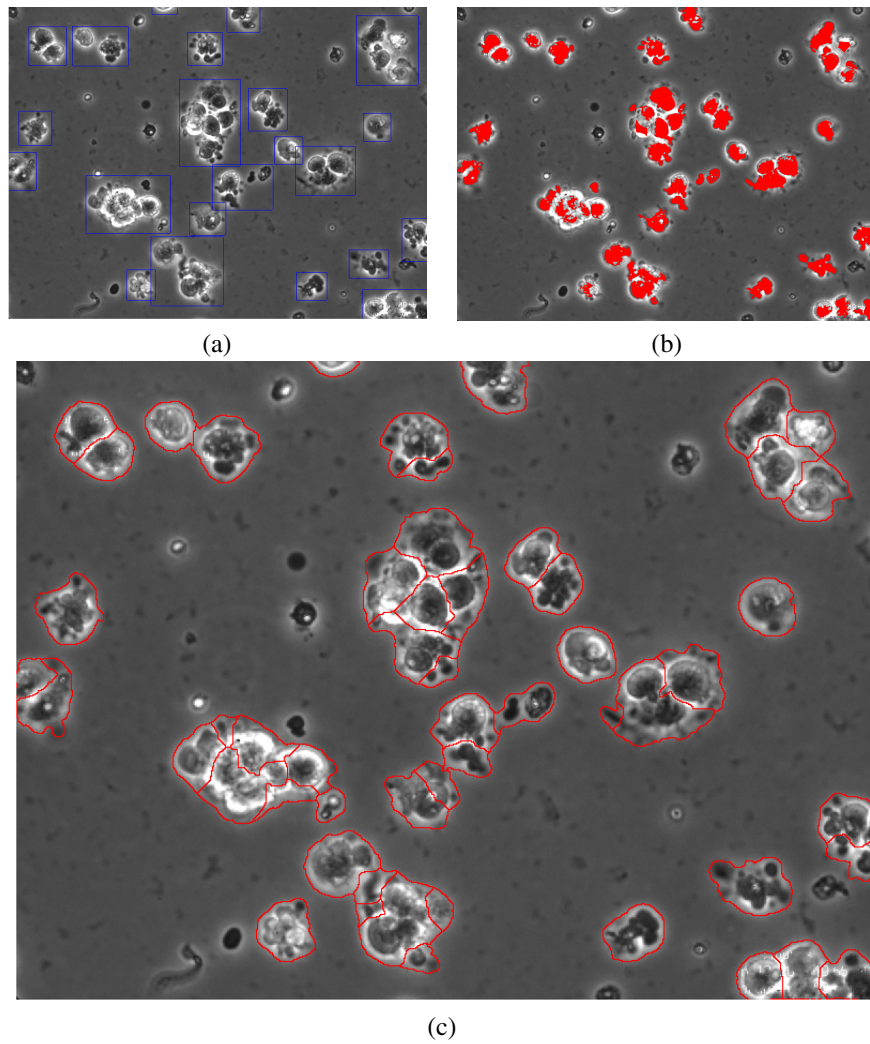


Figure 7: Cell Colony Analysis: (a) Regions of interest, (b) Markers overlaid on the image, (c) Result after cell colony analysis.

IV. EXPERIMENTAL RESULTS

A. Data

We tested our approach on the phase contrast images of Human Embryonic Stem Cell captured with BioStation IM. The images were taken under an objective of $20\times$ with a 800×600 resolution. Each frame from the video is captured roughly every two minutes. Videos 1 and 2 contain more substrate-attached cells and cells that are going through pre-attachment behavior. Videos 3 to 6 have more single unattached cells and cells that are going through apoptosis. In the experiments, we studied the first ten frames of each video.

B. Parameters

To estimate the spatial information image, the scale m is varied from 3 to 25 for each video frame in steps of 2. For each spatial information image, threshold T is varied in steps of 0.5 from the minimum to the maximum of the spatial information image. For all the videos, we use the spatial information from scale $m = 15$ for the selective attenuation before mixture of Gaussians estimation.

C. Mixture of Gaussians

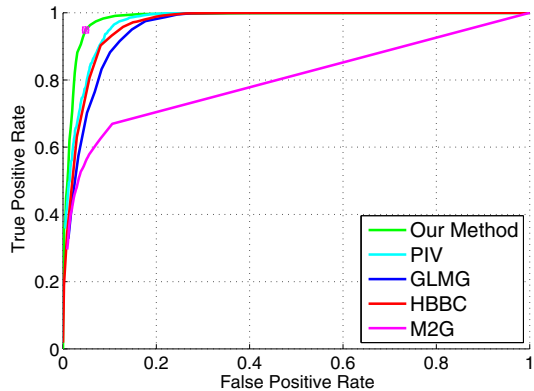
In order to initialize mixture of three Gaussians, we make an initial assumption that there are only two regions of interest in the image: the background and the foreground. The result from the mixture of two Gaussians is then used to estimate the initial weights, means and standard deviations of mixture of Gaussians for three regions of interest. The initial parameters for the mixture of two Gaussians were set as:

$$w_B = 0.5; w_F = 0.5; \mu_B = 64; \mu_F = 192;$$

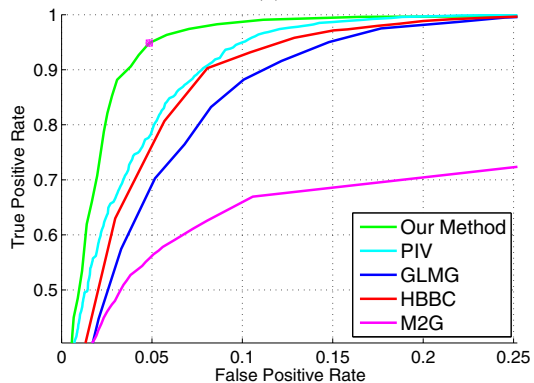
$$\mu = \frac{1}{M \times N} \sum_{r=1}^M \sum_{c=1}^N I_G(r, c) \quad (10)$$

$$\sigma_B = \sigma_F = \sqrt{\frac{1}{M \times N} \sum_{r=1}^M \sum_{c=1}^N (I_G(r, c) - \mu)^2} \quad (11)$$

where, w_B and w_F are the weights, μ_B and μ_F are the means, σ_B and σ_F is the standard deviations of the background and foreground, and μ is the mean of I_G . After the convergence of mixture of two Gaussians, we find the intersection χ between the components. We split the background at $\mu_B - (\chi - \mu_B)$ into substrate-attached cell regions and the substrate. Estimates are generated from these regions to initialize corresponding parameters for the mixture of three Gaussians. The foreground region is directly used to estimate the initial values for the halo region parameters.



(a)



(b)

Figure 10: (a) ROC for all six methods for one of the frames, the magenta square represents the final solution for our method. (b) Zoom-in of top left corner (a).

D. Results

The results of cell region detection achieved by our approach were compared with ground truth labeling conducted by an expert. The average accuracy and false discovery rates for all the videos are reported in Tables I and II respectively.

Table I: Average accuracy

Video	HBBC	GLMG	PIV	M2G	M3G	Our app.
1	0.8251	0.8122	0.8369	0.8703	0.8695	0.9534
2	0.7628	0.8214	0.8528	0.8017	0.8201	0.9311
3	0.8584	0.8102	0.8449	0.9116	0.9039	0.9562
4	0.8768	0.8613	0.8556	0.9308	0.9175	0.9482
5	0.8913	0.8577	0.8708	0.9272	0.9174	0.9491
6	0.8631	0.8172	0.8332	0.9116	0.8988	0.9571

Table II: Average false discovery rate

Video	HBBC	GLMG	PIV	M2G	M3G	Our app.
1	0.4745	0.4944	0.4605	0.2116	0.2894	0.1612
2	0.4792	0.4054	0.3620	0.2065	0.2345	0.1732
3	0.4635	0.5377	0.4868	0.2585	0.3211	0.2006
4	0.4698	0.4996	0.5097	0.2704	0.3484	0.2661
5	0.4058	0.4743	0.4508	0.2341	0.3043	0.2335
6	0.4204	0.4939	0.4705	0.2267	0.3021	0.1724

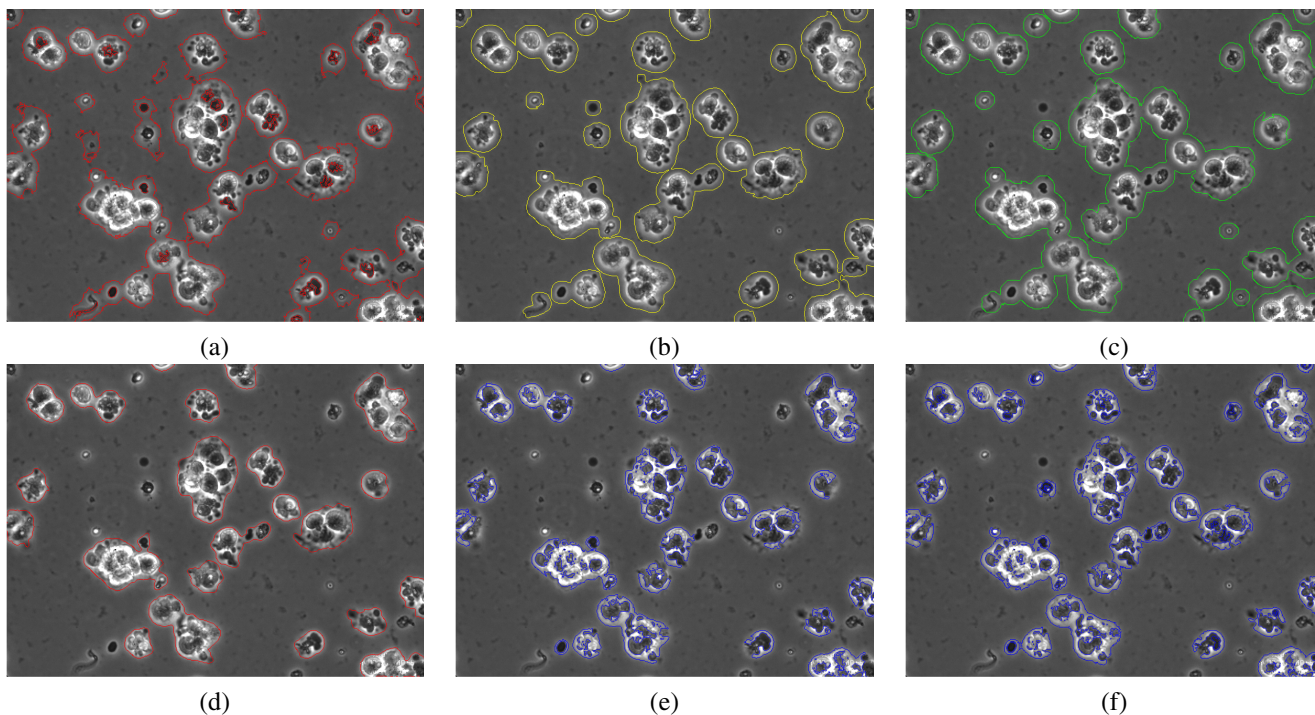


Figure 8: Comparison with related work: (a) Detection by histogram based Bayesian classifier, (b) Detection by pixel intensity variance, (c) Detection by gray level morphological gradient, (d) Detection by our method, (e) Detection by mixture of two Gaussians, (f) Detection by mixture of three Gaussians.

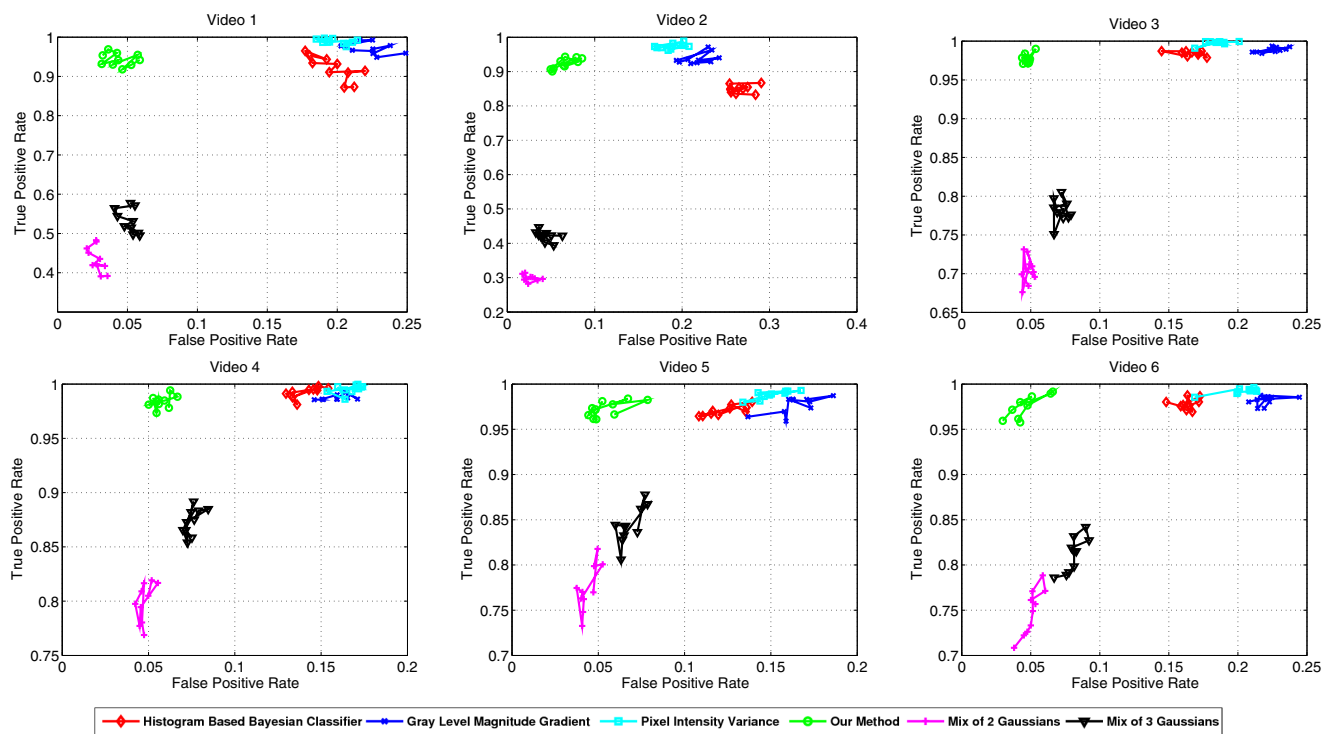


Figure 9: Cost and benefit plots of videos 1 to 6 for different methods.

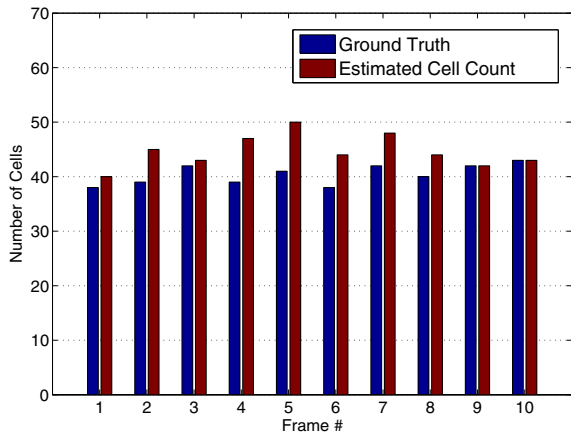


Figure 11: Comparison of estimated cell counts with the actual cell counts for video 1.

For comparison, we implemented PIV, GLMG and histogram based Bayesian classifier (HBBC) detection methods. The result of our method and these methods are shown in Figs. 8(a) to (d). We can see that the overestimation of cell regions is a major problem for the PIV, GLMG and HBBC methods. Moreover, detection by PIV and GLMG require a user defined threshold to determine whether a pixel belongs to the cell region or to the substrate. The HBBC method is more tedious compared to other methods since it requires ground truth for the cell regions for training of the classifier. Our method needs only an initial scale to estimate the spatial information image for selective attenuation and a largest allowable scale that is to be used for optimization. In addition, we compare our approach with the outcome from the mixture of two and three Gaussians as shown in Figs. 8(e) and (f) respectively. The performance of all the six methods is summarized in Tables I and II. Table II shows that our method has a consistent low false discovery rate. The low false discovery rate for mixture of Gaussians is due to the underestimation of cell regions by the method. Table I shows that our approach yields higher accuracy in cell region detections compared to other methods. The cost (False positives) and benefit (True positives) statistics for all six videos is shown in Fig. 9. As one can see, our method has a high true positive rate while maintaining a low false positive rate for all six videos. Figures 10(a) and (b) show the ROC plots for all the methods discussed in this paper and our method outperforms all other methods. Figure 11 shows the cell count results compared to the cell count ground truth. Although the cell counts are satisfactory, the current method overestimates the count.

V. CONCLUSIONS

In this paper, we proposed a cell region detection method by using spatial information and mixture of Gaussians model. This method gives tight boundaries for cell regions. The method can be used for individual cell detection with

the local markers found by the mixture of Gaussians. Experiments were carried out to test the method for cell region detection and the results show that it provides a better detection accuracy than the other methods in literature. In the future, our work will focus on further improving the cell colony analysis by developing a new marker detection method. We will also look into developing a tracking system for the HESCs.

ACKNOWLEDGMENT

This work is supported by the NSF Integrated Graduate Education Research and Training (IGERT): Video Bioinformatics Grant DGE 0903667.

REFERENCES

- [1] R. Yu, M. Wu, S. Lin, and P. Talbot, "Cigarette Smoke Toxicants Alter Growth and Survival of Cultured Mammalian Cells," *Toxicological Sciences*, vol. 93, no. 1, pp. 82–95, 2006.
- [2] Biostation-IM. [Online]. Available: <http://www.nikoninstruments.com/Vyrobky/Cell-Incubator-Observation/BioStation-IM>
- [3] M. Stojkovic, M. Lako, T. Strachan, and A. Murdoch, "Derivation, growth and applications of human embryonic stem cells," *Reproduction*, vol. 128, no. 3, pp. 259–267, 2004.
- [4] K. Li, M. Chen, and T. Kanade, "Cell population tracking and lineage construction with spatiotemporal context," in *Proceedings of the 10th International Conference on Medical Image Computing and Computer-Assisted Intervention (MICCAI)*, 2007, pp. 295 – 302.
- [5] O. Fackler and R. Grosse, "Cell motility through plasma membrane blebbing," *J Cell Biol.*, vol. 181, no. 6, p. 879884, 2008.
- [6] F. Ambriz-Colin, M. Torres-Cisneros, J. Avina-Cervantes, J. Saavedra-Martinez, O. Debeir, and J. Sanchez-Mondragon, "Detection of biological cells in phase-contrast microscopy images," in *Artificial Intelligence, 2006. MICAI '06. Fifth Mexican International Conference on*, 2006, pp. 68 –77.
- [7] D. A. Forsyth and J. Ponce, *Computer Vision: A Modern Approach*. Prentice Hall Professional Technical Reference, 2002.
- [8] A. P. Dempster, N. M. Laird, and D. B. Rubin, "Maximum likelihood from incomplete data via the EM algorithm," *Journal of the Royal Statistical Society. Series B (Methodological)*, vol. 39, no. 1, pp. pp. 1–38, 1977.
- [9] S. Gopinath, Q. Wen, N. Thakoor, K. Luby-Phelps, and J. X. Gao, "A statistical approach for intensity loss compensation of confocal microscopy images," *Journal of Microscopy*, vol. 230, no. 1, pp. 143–159, 2008.
- [10] F. Cloppet and A. Boucher, "Segmentation of complex nucleus configurations in biological images," *Pattern Recogn. Lett.*, vol. 31, pp. 755–761, June 2010.